Experimental study on electrical resistivity measurement of a specimen at high temperature

Chunsuo Xin (辛春锁)[1,2*], Jingmin Dai (戴景民)[1], and Xiaowa He (何小瓦)[2]

[1] *Department of Automation Measurement and Control, Harbin Institute of Technology, Harbin 150001, China*

[2] *Aerospace Research Institute of Materials and Processing Technology, Beijing 100076, China*

[*] *E-mail: xinchun_cn@yahoo.cn*

Received September 27, 2008

A new technique is developed to measure the electrical resistivity of conductor with a nonuniform temperature profile. The calculation method is derived from the temperature dependence of the electrical resistivity. The apparatus consists mainly of a high temperature environmental chamber, a power circuit of heating, a twenty-wavelength pyrometer, and a scanning pyrometer. After getting the resistance from the voltage drop of the specimen, the electrical resistivity in a wide temperature range of the specimen can be obtained by our calculation model. Preliminary results of the electrical resistivity of SRM 8424 over a wide temperature range (1000−3000 K) are presented. The perfect consistency between the measurement results and the nominal values justifies the validity of this technique.

OCIS codes: 120.0120, 120.4570, 000.6850, 120.6780.

doi: 10.3788/COL20090707.0585.

Electrical resistivity is one of the important thermophysical properties. The corresponding value of electrical resistivity at different temperatures is not only used to study the characteristic of the material, but also to instruct the production of new materials. The measuring method of electrical resistivity generally relies on the current heating technique which can be computed by the Ohm's Law[1,2]. The measuring precision of the current heating technique depends mainly on the degree of keeping uniform temperature of the specimen, which is hard to be realized because of thermal conduction at ends, especially at high temperatures. Nonuniform temperature profile restricts the application of this method at ultra high temperatures. With the development of pulse heating method and the modern electronics, Righini *et al*. at the Istituto di Metrologia (IMGC) proposed a new idea to measure the thermophysical properties by an assumed function of thermophysical properties and temperature according to the rules of thermophysical varying with temperatures[3]. They developed a method to measure the thermal expansion of a specimen with a non-uniform temperature profile[3]. As an extension of Righini's idea, we propose a new method for measuring the electrical resistivity of a specimen with a non-umiform temperature profile. Using a multi-thermophysical property measurement apparatus and a high-speed scanning pyrometer, the experiments for measuring the electrical resistivity of SRM 8424 at a ultra high temperature are implemented.

The specimen, which must be an electrical conductor, is heated from room temperature to a high temperature and kept at steady state at last by Joule heating with a current. For thermal conduction and radiation, the specimen may have a nonuniform temperature distribution. If the temperatures are measured in positions z_1, z_2, $\cdots$, z_M with equal intervals, the specimen may be thought as composed of M segments with equal length of S. These segments are marked as l_i ($i = 1, 2, \cdots, M$) and the corresponding length at temperature T_0 may be of any size and they are not necessarily equal.

As a segment of the specimen, the function of the temperature-dependent resistance may be represented by an n-order polynomial constrained to a reference temperature T_0[4]:

$$\begin{aligned} q(T_i) &= \frac{R_i(T_i) - R_i(T_0)}{R_i(T_0)} \\ &= a_1 \cdot (T_i - T_0) + a_2 \cdot (T_i - T_0)^2 \\ &+ \cdots + a_n \cdot (T_i - T_0)^n, n = 1, 2, \cdots, \end{aligned} \tag{1}$$

where $R_i(T_0)$ is the resistance of the segment at room temperature, and $R_i(T_i)$ is the corresponding quantity at a high temperature T_i, and T_i is the average temperature associated with the specimen segment between positions z_i and z_{i+1}. Equation (1) can be rewritten as

$$R_i(T_i) - R_i(T_0) = q(T_i) \cdot R_i(T_0), i = 1, 2, \cdots, M. \tag{2}$$

For Eq. (2) is valid to any segment of the specimen, based on the Ohm's Law, the sum of all segments gives

$$R(T) - R(T_0) = \frac{S \cdot \rho(T_0)}{A} \sum_{i=1}^{M} \frac{q(T_i)}{1 + T_i \cdot \alpha(T_i)}, \tag{3}$$

where $R(T)$ is the total resistance with a nonuniform temperature profile T, $R(T_0)$ and $\rho(T_0)$ are the total resistance and the electrical resistivity of the specimen at room temperature respectively, $\alpha(T_i)$ is the thermal expansion coefficient of the specimen at T_i, which is defined as $\alpha(T_i)=(S-l_i)/(T_i.l_i)$.

Equation (3) can be rewritten as

$$\frac{R(T)-R(T_0)}{S\cdot\rho(T_0)/A}=a_1\sum_{i=1}^{M}\frac{T_i-T_0}{1+T_i\cdot\alpha(T_i)}+a_2\sum_{i=1}^{M}\frac{(T_i-T_0)^2}{1+T_i\cdot\alpha(T_i)}+\cdots+a_n\sum_{i=1}^{M}\frac{(T_i-T_0)^n}{1+T_i\cdot\alpha(T_i)},\quad n=1,2,\cdots. \tag{4}$$

Since Eq. (4) is valid to any profile, it may be rewritten when applied to the generic kth profile as

$$\frac{R_k(T)-R_k(T_0)}{S_k\cdot\rho(T_0)/A}=a_1\sum_{i=1}^{M_k}\frac{T_{ki}-T_0}{1+T_{ki}\cdot\alpha(T_{ki})}+a_2\sum_{i=1}^{M_k}\frac{(T_{ki}-T_0)^2}{1+T_{ki}\cdot\alpha(T_{ki})}+\cdots+a_n\sum_{i=1}^{M_k}\frac{(T_{ki}-T_0)^n}{1+T_{ki}\cdot\alpha(T_{ki})},\quad n=1,2,\cdots, \tag{5}$$

where M_k is the segment at the kth experiment.

The specimen may have an arbitrary temperature distribution. An overdetermined system may be got if p profiles are measured:

$$\begin{bmatrix}\frac{R_1(T)-R_1(T_0)}{S_1\cdot\rho(T_0)/A}\\ \vdots\\ \frac{R_p(T)-R_p(T_0)}{S_p\cdot\rho(T_0)/A}\end{bmatrix}=\begin{bmatrix}\sum_{i=1}^{M_1}\frac{(T_{1i}-T_0)}{1+T_{1i}\cdot\alpha(T_{1i})},\sum_{i=1}^{M_1}\frac{(T_{1i}-T_0)^2}{1+T_{1i}\cdot\alpha(T_{1i})},\cdots,\sum_{i=1}^{M_1}\frac{(T_{1i}-T_0)^n}{1+T_i\cdot\alpha(T_{1i})}\\ \vdots\quad\cdots\quad\vdots\\ \sum_{i=1}^{M_p}\frac{(T_{pi}-T_0)}{1+T_{pi}\cdot\alpha(T_{pi})},\sum_{i=1}^{M_p}\frac{(T_{pi}-T_0)^2}{1+T_{pi}\cdot\alpha(T_{pi})},\cdots,\sum_{i=1}^{M_p}\frac{(T_{pi}-T_0)^n}{1+T_{pi}\cdot\alpha(T_{pi})}\end{bmatrix}\times\begin{bmatrix}a_1\\ a_2\\ \vdots\\ a_n\end{bmatrix}, \tag{6}$$

where M_p is the segments at the pth experiment.

The parameters a_1, a_2, $\cdots$, a_n may be obtained by the least square techniques when $p>n$. Since electrical resistivity functions are generally well represented by low degree polynomials, and a few profiles are sufficient for an overdetermined system.

At the same time, Eq. (1) may be rewritten according to the Ohm's Law as

$$q(T_i)=\frac{\rho_i(T_i)\cdot[1+T_i\cdot\alpha(T_i)]-\rho(T_0)}{\rho(T_0)}. \tag{7}$$

Consequently, the electrical resistivity after correcting the thermal expansion can be calculated by

$$\rho_i(T_i)\cdot[1+T_i\cdot\alpha(T_i)]=\rho_i(T_0)\cdot\left[1+a_1(T_i-T_0)+a_2(T_i-T_0)^2+\cdots+a_n(T_i-T_0)^n\right],\quad n=1,2,\cdots, \tag{8}$$

where $[1+T_i\cdot\alpha(T_i)]$ is the correcting factor of thermal expansion.

Experiments were performed with the apparatus developed for multi-thermophysical-property measurements[5] with some modifications. The apparatus was composed of an electric power circuit, an environmental chamber, two pyrometers, a high-speed data acquisition system, and various associated components[6]. A block diagram of the experimental apparatus is shown in Fig. 1. The power circuit included the specimen in series with two graphite electrodes, a standard resistor, and a switching power. The specimen was screwed to the electrodes. The maximum heating temperature is determined by the radius of the specimen, and the profile may be changed with different dimensions of graphite electrodes. Brass electrodes were fixed at the experimental chamber for electric connection and heat conduction. In order to reach a steady state and provide steep temperature gradients toward the ends of the specimen, chilled water was circulated in the interior of the brass electrodes. A standard resistance (1 mΩ) was used to measure the heating current through the specimen. The switching power was computer operated through metal oxide semiconductor field effect transistor (MOSFET) drivers with a predetermined time.

The experimental chamber contained the specimen, two graphite electrodes, an expansion joint, voltage probes, and a radiation shield. The specimen was encircled by a radiation shield which was made of 30-mm-thick carbon felt in order to absorb the radiant energy emitted by the sample. An expansion joint allowed the expansion of the specimen in the upper direction. The voltage probes were knife edges made of the specimen

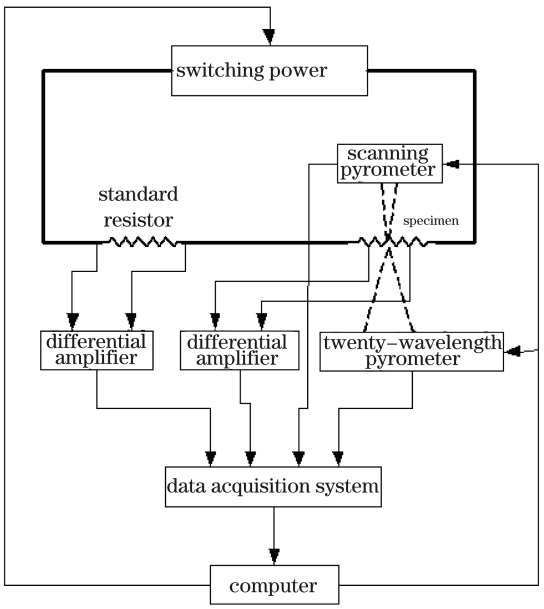

Fig. 1. Block diagram of the experimental apparatus.

material and placed at a distance approximately 10 mm from the end graphite electrode. The frame of the chamber was made of stainless steel and sealed at the front and back sides by two doors with fused-silica windows for temperature measurement. The experiments of electrical resistivity were performed by means of double-wall water-cooling to make sure that the heat from the hot zone was absorbed by the chamber walls at room temperature. A vacuum pump system was necessary to avoid the oxidation of the sample and graphite electrodes at ultra high temperatures. The minimum achieved pressure of the vacuum was 1.7×10^{-3} Pa using the fore-pumping system, which consisted of an oil-free mechanical pump and two molecular-sieve absorption pumps.

Radiation thermometry is an excellent method to quickly measure the temperature of an object without contact[7]. The true temperature and spectral emissivity of the fixed part may be got by a twenty-wavelength pyrometer[8], which was placed at the front of the specimen and operated at the center of the specimen. The optical system of a pyrometer is very important to its quality and intrinsic characteristics. The scheme is shown in Fig. 2. The optical system of the pyrometer consists of optical collection part, optical fiber, and prism splitting part. The optical collection part was used to aim, and the aiming accuracy within the limit of one square millimeter was guaranteed by a forty-time optical acquisition system. The energy was transferred to the prism splitting part through an optical fiber and refracted. At last, the light was received by the corresponding detectors. There are many advantages to transmit radiation energy by optical fiber from optical collection part to prism splitting part on long-distance. For example, it can improve the stability of pyrometer working in bad environment and expand the application scope[9]. The working wavelength of the twenty-wavelength pyrometer was from 0.4 to 1.1 μm, and its measuring accuracy of spectral emissivity was higher than 90%. The pyrometer covered a temperature range from 1000 to 3800 K using an auto-ranging feature, and the fastest response time of the pyrometer was 10 μs. The upper limit was determined by the possible maximum heating range of the specimen. The lower limit of measuring temperature was determined by the conditions of the pyrometer and the radioactive properties of the specimen. The measuring error of the pyrometer was less than 1%. The longitudinal temperature profiles of the specimen were obtained by a scanning pyrometer placed at the opposite position to the twenty-wavelength pyrometer. The scanning pyrometer consisted of a fiber color pyrometer and a scanning system[10−12]. The fiber color pyrometer and the twenty-wavelength pyrometer had the same structure and parameters but with different working wavelengths, the former worked at 0.656 and 0.9 μm. The scanning system consisted of a fixed mirror and a rotating mirror with associated electronics, as shown in Fig. 3. Radiation from different points on the specimen was received by the rotating mirror, which reflected the radiation to the fixed mirror and then to the color pyrometer optics. A rectangular rotating mirror was mounted in a steel support with the rotation axis located in the reflecting surface. The maximum scanning angle of the rotating mirror was limited to 40° by an eccentric

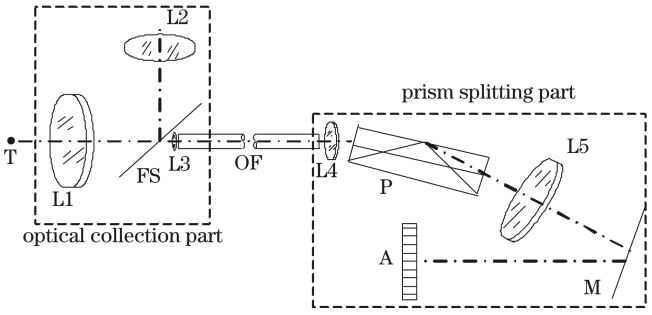

Fig. 2. Optical scheme of twenty-wavelength high-speed pyrometer. T: target; L1: objective lens; L2: eyepiece; FS: field stop; L3: condenser lens; OF: optical fiber; L4: collimating lens; P: prism; L5: camera obscura objective; M: optical reflector; A: photodetector.

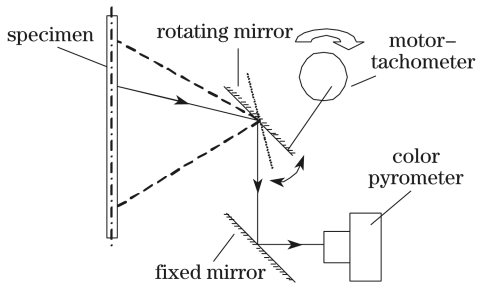

Fig. 3. Frame scheme of scanning optical detector.

wheel, which was driven by a motor-tachometer with an external feedback control loop to stabilize the rotation. The entire equipment was fixed on a steel shell and statically balanced to assure a smooth rotation. In order to control other irradiation from the environment and reduce multiple-reflection of radiation between the sample surface and surroundings, the surface of the shell was coated by a black paint, whose spectral emissivity was superior to 0.93 in the infrared region.

The data corresponding to temperature, current, and voltage were recorded with a high-speed digital data acquisition system, which consisted of a multiplexer, analog-to-digital (A/D) converter, digital-to-analog (D/A) converter, and interfacing equipment. The multiplexed signals went to the A/D converter, which had a full-scale reading of ±10 V and a full-scale resolution of one part was 2^{16}=65536. The typical data acquisition rate of these data was 100 kHz. The data acquisition system was controlled by a computer, and the recorded data were transferred to the computer for storing and processing. Another function of the computer was controlling the working state of the switching power.

Several measurements of electrical resistance were performed on a cylinder graphite with two gauges. The specimen made of SRM 8424 was processed at Harbin Institute of Technology. The 'start' and 'end' positions of the specimen, determined by the gauges, where the measured profiles were used to intercept some of the radiation emitted by the specimen. The electrical resistivity at room temperature was measured with volt-amp method. The laboratory was air-conditioned to keep constant room temperature. Ten minutes after the specimen was

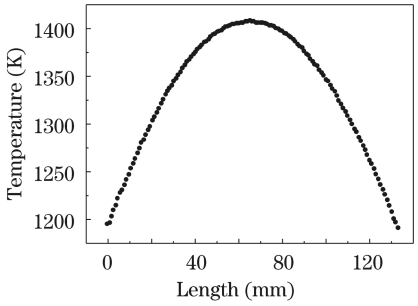

Fig. 4. Typical temperature profile in an electrical resistivity experiment.

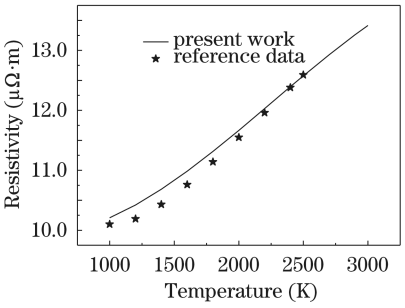

Fig. 5. Temperature dependence of the electrical resistivity.

Table 1. Uncertainties in Measured and Computed Quantities

Measurement	Uncertainty	
	1500 K	2500 K
Temperature Profiles		
Scanning System	1 K	3 K
Transformation of Radiance Temperature into True Temperature	15 K	25 K
Combined Temperature Uncertainty	15 K	25.2 K
Corresponding Uncertainty in Electrical Resistivity	0.21%	0.36%
Electrical Resistance		
Voltage	2%	
Current	2%	
Thermal Expansion	1%	
Combined Uncertainty in Electrical Resistivity	3%	
Overall Uncertainty	3.01%	3.02%

mounted, the chamber was evacuated down to 10^{-3} Pa and purged with argon gas (at ∼1.2 Pa). Such procedures were repeated for three times to minimize the problems associated with specimen oxidation and evaporation at ultra high temperature. Then the chamber was floated with argon gas and the sample was heated in steps of 300−400 K. The specimen was regarded as gray when the measured emissivities in equilibrium states on the central point were higher than 0.89. The measured temperature differences between twenty-pyrometer and the maximum data of scanning pyrometer were less than 5 K. Therefore, radiance temperature measurements of the scanning pyrometer were deal as true temperatures. Several temperature profiles were got at the equilibrium state, which can be judged from the outputs of the twenty-wavelength pyrometer. Figure 4 shows the typical shape of temperature profiles. Several temperature profiles and corresponding resistances were recorded to calculate the function of electrical resistivity at high temperature with the method described above. The fitted function of the electrical resistivity ρ, which is corrected for thermal expansion in the range from 1000 to 3000 K, is given by

$$\rho = 10.17071 - 1.05 \times 10^{-3}T + 1.27587 \times 10^{-6}T^2 - 0.188426 \times 10^{-9}T^3. \quad (9)$$

Compared with traditional measuring techniques, the maximum advantage of the technique lies in less measuring procedures and larger numbers of electrical resistivity in the range from 1000 to 3000 K. Figure 6 shows the typical curve of the electrical resistivity versus temperature. The electrical resistivity of the present work gradually increases with increasing temperature, which is consistent with the results supported by the National Institute of Standards and Technology (NIST) of USA. The maximum error of the electrical resistivity occurs at 1200 K because of the less overlapping profiles at lower temperature range.

The measurement uncertainty sources include the measurements of temperature, the drop of voltage, the current, and the thermal expansion. Their estimated uncertainties at 1500 and 2500 K are reported in the Table 1.

For temperature profile measurements, the uncertaing comes from the following cases. 1) Spatial positions on the specimen that may be wrong due to the uncertainties of mirror-specimen geometry or the small rotational speed changes during the profile measurement. 2) The error caused by the transformation between the true temperatures and the radiance temperatures which are measured by the scanning pyrometer. 3) The electrical resistance computed errors which are caused by the measurement error of voltage and current. The thermal expansion coefficients of the specimen at different temperatures are commended data of NIST.

In conclusion, the experimental apparatus was constructed and measurements were performed to measure the electrical resistivity of SRM 8424. Our approach is a transformation of the current heating method (steady state) in which the electrical resistivity of a long specimen with a nonuniform temperature profile is measured. The perfect consistency between the present and reference results justifies that our technique is capable of measuring the electrical resistivity in the range from 1000 to 3000 K. The uncertainty of the present work is about 3%.

The apparatus was designed mostly for use in C/C composites, but it can also be partly used for metals and semiconductors such as ceramics. Furthermore, the proposed method can measure simultaneously the electrical resistivity, thermal expansion, hemispherical total emissivity, and normal spectral emissivity of the same sample under the same experimental conditions.

This work was supported by the General Armament Department under Grant No. 51312060201.

References

1. A. Cezairliyan, Int. J. Thermophys. **5,** 177 (1984).
2. D. D. L. Chung, J. Therm. Anal. Calorim. **65,** 153 (2001).
3. F. Righini, J. Spišiak, G. C. Bussolino, and F. Scarpa, High Temp. High Press. **29,** 473 (1997).
4. F. Righini, R. B. Roberts, A. Rosso, and P. C. Cresto, High Temp. High Press. **18,** 561 (1986).
5. J. Dai, C. Xin, and X. He, Chin. Opt. Lett. **6,** 669 (2008).
6. P. Xiao, J. Dai, and Q. Wang, Chin. Opt. Lett. **5,** 642 (2007).
7. H. W. Yoon, C. E. Gibson, V. Khromchenko, G. P. Eppeldauer, R. R. Bousquet, S. W. Brown, and K. R. Lykke, Int. J. Thermophys. **29,** 285 (2008).
8. C. Xin, J. Dai, and Y. Wang, Infrared Technol. (in Chinese) **30,** 47 (2008).
9. L. Liu, J. Wang, L. Xin, X. Jiang, and P. Li, Chin. J. Sci. Instrum. (in Chinese) **24,** 547 (2003).
10. C. Xin, J. Dai, X. He, and L. Huang, Laser and Infrared (in Chinese) **38,** 219 (2008).
11. L. Su, W. Zhao, X. Hu, D. Ren, and X. Liu, Chin. Opt. Lett. **5,** 609 (2007).
12. F. Righini, R. B. Roberts, and A. Rosso, High Temp. High Press. **18,** 573 (1986).